Enhanced Configurational Sampling in Binding Free-Energy Calculations

Christopher J. Woods and Jonathan W. Essex*

Department of Chemistry, University of Southampton, Highfield, Southampton, SO17 1BJ, United Kingdom

Michael A. King

Celltech Group plc, 208 Bath Road Slough, SL1 3WE, United Kingdom

Received: July 24, 2003; In Final Form: October 3, 2003

The newly developed method of replica-exchange thermodynamic integration (RETI) was tested and compared with finite-difference thermodynamic integration (FDTI) on the calculation of the relative binding free energies of halides to a calix[4]pyrrole derivative. The calculation was challenging, because the dimethylsulfoxide solvent was contaminated by small amounts of water. The λ-swap move of RETI enabled more-complete sampling of the solvents and produced relative binding free energies that included the effect of the fluoride's higher affinity for water. In addition, the λ-swap move increased the quality of the configurational sampling of the host, because the system was able to escape from local minima. The results demonstrate that the sampling of RETI is superior to that of FDTI, at no additional computational expense.

1. Introduction

The efficient calculation of relative binding free energies in an explicit solvent is the primary focus of many condensed-phase simulations.[1] Such calculations are complicated by the many degrees of freedom that the explicit solvent introduces and the frustrated energy surfaces that result from the solvent−solvent interactions. These frustrated energy surfaces lead to poor sampling, because the system may become trapped within local minima. Recently, a new free-energy method—replica-exchange thermodynamic integration[2] (RETI)—was developed that improved the quality of solvent configurational sampling.[2] It is the purpose of this paper to apply RETI to the challenging calculation of relative binding free energies in a mixed-solvent system, and to compare the results and sampling produced with those from finite-difference thermodynamic integration (FDTI).[3−7]

2. Theory

Relative binding free energies may be calculated via the free-energy cycle[1,8] shown in Figure 1. The calculation itself consists of two separate simulations: one that perturbs one guest into another while bound to the host (the bound leg), and one that perturbs one guest into another while they are free in the solvent (the free leg). Many methods are available for calculating the relative free energy of each leg.[1,8,9] Most of these methods use a λ-coordinate to perturb one guest into another gradually. For example, if the relative free energy was desired between guests A and B, then λ would be used to scale the force field of the system such that it represented guest A at $\lambda = 0.0$, guest B at $\lambda = 1.0$, and a nonphysical hybrid of A and B at intermediate values.

FDTI[3−7] is one of the methods available to calculate the free energy across λ. FDTI is a version of thermodynamic integration (TI)[10−12] that calculates the gradient of the free energy with respect to λ, $(\partial G/\partial\lambda)_\lambda$, and then integrates the gradient across λ to obtain the relative free energy. FDTI approximates the free-energy gradient $(\partial G/\partial\lambda)_\lambda$ with the finite difference $(\Delta G/\Delta\lambda)_\lambda$, which may be calculated via the Zwanzig equation:[13]

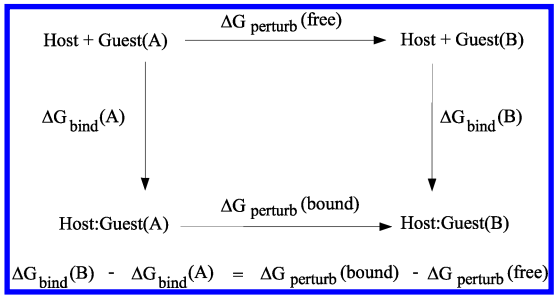

Figure 1. Free-energy cycle used to calculate the relative binding free energy of guests A and B to a host.

$$\Delta G_{\lambda\rightarrow\lambda+\Delta\lambda} = -kT \ln \left\langle \exp\left(-\frac{E_{\lambda+\Delta\lambda} - E_\lambda}{kT}\right)\right\rangle_\lambda \qquad (1)$$

where E_λ is the energy of the system, k the Boltzmann's constant, and T the simulation temperature. The symbols $\langle ... \rangle_\lambda$ indicate that the average is formed over the ensemble generated at λ. Double-wide sampling[14] may be used to estimate both a forward ($\lambda \rightarrow \lambda + \Delta\lambda$) and backward ($\lambda \rightarrow \lambda - \Delta\lambda$) free-energy gradient. Assuming that $\Delta\lambda$ is sufficiently small, then the magnitude of both of these should be equal, and the finite difference is a good approximation of the true free-energy gradient.

RETI[2] is an extension of FDTI that combines it with Hamiltonian replica- exchange[15,16] (Figure 2).

The simulation is conducted in the standard manner, with a replica of the system at each value of λ. Unlike standard FDTI, there is the addition of a periodic λ-swap move, whereby neighboring λ-replicas are tested according to the Hamiltonian replica-exchange test. This test is the same for the NVT and

* Author to whom correspondence should be addressed. E-mail: J.W.Essex@soton.ac.uk.

10.1021/jp036162+ CCC: $25.00
Published on Web 11/14/2003

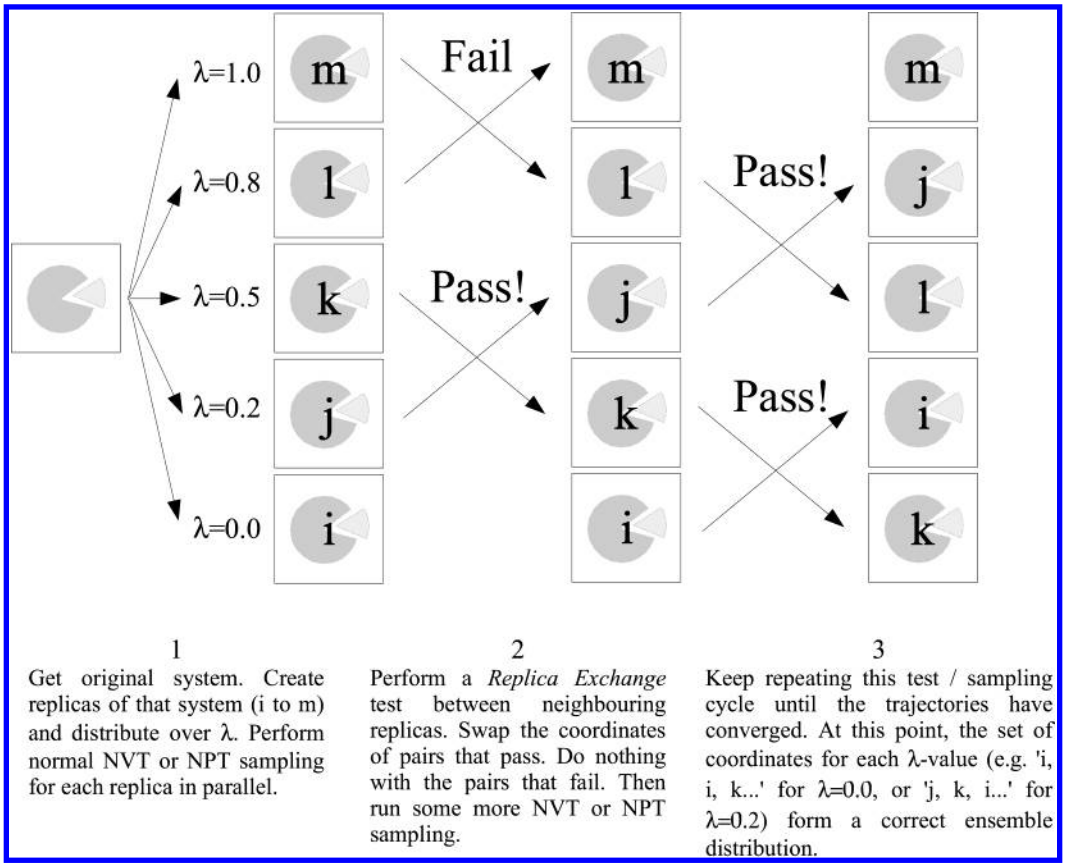

Figure 2. Schematic of the replica-exchange thermodynamic integration (RETI) algorithm.

NPT ensembles. For replica i at λ = A and energy $E_A(i)$, and replica j at λ = B and energy $E_B(j)$, the test is given by

$$\exp\left[\frac{1}{kT}(E_B(j) - E_B(i) - E_A(j) + E_A(i))\right] \geq \text{rand}(0, 1) \qquad (2)$$

where rand(0, 1) represents a uniform random number generated from $0.0 \leq \text{rand}(0, 1) \leq 1.0$.

If this test is passed, then the coordinates of the pair of λ values are swapped. The derivation of this test[16] is similar to that used for parallel tempering (PT).[17,18] It is useful to note that this test is just the product of two normal Metropolis tests: one going from configuration i to j at λ = A, and the other going from j to i at λ = B. The replica-exchange test is the product of these tests, because both moves must occur simultaneously.

This sampling-test iteration is continued until convergence. At this point, the set of trajectories at each value of λ form a correct ensemble distribution for that value of λ, and, thus, the free-energy average is formed correctly. The advantages of this method are that it is almost trivial to implement, with the addition of an inexpensive λ-swap move and test, and the additional bookkeeping needed to keep track of which trajectories are at what λ values. In addition, this scheme allows each trajectory to move freely across λ, leading to improved configurational sampling and a reduction in random sampling error.[2]

3. Experimental Section

3.1. Test System. The system chosen for the testing of RETI on mixed-solvent systems was the binding of halide ions to a calix[4]pyrrole derivative[19,20] (Figure 3).

This system is of experimental interest because it has been shown that the host specifically binds fluoride ions when

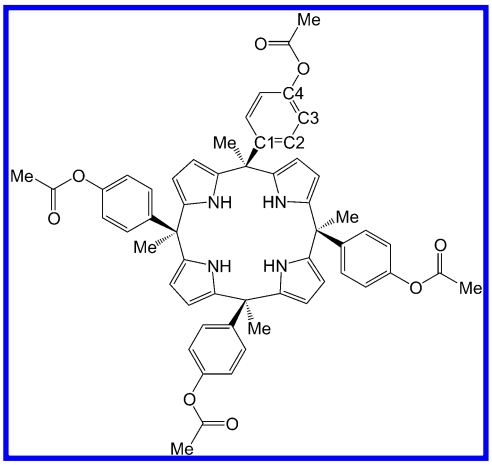

Figure 3. Schematic of the derivative investigated in this study.

solvated by dimethylsulfoxide (DMSO).[20] Our recent work simulating this system[20] has demonstrated that the host's high affinity for fluoride ions is reduced by the presence of contaminating water. This conclusion, which is in agreement with the theoretical observations of other workers,[21] was based on the running of simulations that manually positioned water molecules into hydrogen-bonding geometries with the halide, and observing the resulting effect on the relative binding free energies. The contaminating water had to be positioned manually, as the restricted sampling of the solvent led to its poor mobility over the time scale of the simulations. The primary intent of this work was to investigate whether RETI could sample from many different water distributions without a need for manual intervention and, in so doing, include the effect of increased fluoride affinity for water into the relative binding free-energy results.

Our previous work on the calix[4]pyrrole−halide system[20] tested and compared both free-energy perturbation[13,22−24] (FEP) and adaptive umbrella weighted histogram analysis method (AdUmWHAM).[25,26] The study concluded that the dynamic λ-coordinate of AdUmWHAM led to greater configurational sampling of the host. RETI also uses a dynamic λ-coordinate, through the use of the λ-swap move. Therefore, the secondary intent of this study is to investigate whether the use of a dynamic λ-coordinate leads to RETI, also exhibiting greater configurational sampling of the host.

3.2. Simulation Conditions. The internal coordinate Z-matrix of the host was built using the fragment approach of van Hoorn and Jorgensen,[27] and their parameters were used for the macrocycle ring.[27] Generic OPLS[28,29] parameters were used for the pendant arms and the halides. The Z-matrix and parameters for this system are given in the supporting information of Woods et al.[20] The crystal structure[20] configuration of the calix[4]-pyrrole−fluoride complex was solvated by an orthorhombic box of 631 OPLS DMSO[30] molecules, with initial dimensions of 42.7 Å × 43.6 Å × 49.9 Å. To model the contaminating water, 30 TIP4P[31] water molecules were placed randomly into this box and the system was equilibrated for 1 million (1 M) Monte Carlo (MC) steps under NPT periodic boundary conditions. The equilibration, and all subsequent simulations, were performed in a modified version of MCPRO 1.5.[32] The modifications allowed the code to run a range of different free-energy methods and were checked to ensure that they did not interfere with the normal running of the code. The nonbonded cutoffs were set to 15 Å, the temperature was 25 °C, and the pressure used was 1 atm. The nonbonded interactions were calculated such that if any host atom was within the cutoff, then the interactions with the entire host were calculated. Preferential sampling of the solvent,[33,34] as implemented in MCPRO,[32] was used, with a preferential sampling contant of 200.0 Å and the preferential sampling center on the fluoride.

The free leg of the calculation was constructed using a single fluoride ion placed in the center of an orthorhombic box of 640 DMSO molecules, and 30 randomly positioned TIP4P molecules, with initial dimensions of 44.8 Å × 44.0 Å × 45.8 Å. This system was also equilibrated for 1 M steps under conditions identical to those of the bound leg.

Three mutations were considered; fluoride to chloride, fluoride to bromide, and chloride to bromide. Both the bound and free legs of each mutation were conducted over 21 values of λ, spread evenly across λ every 0.05 units. The final structure from equilibration was used as the starting structure for each λ value for each mutation. To investigate the effect of the contaminating water, the water molecules were repositioned randomly in each of the different λ-replicas, and each replica was alloted another 0.9 M steps to equilibrate to the new water distribution and the new λ value.

The free energy was calculated via FDTI and RETI. Both methods used identical simulation lengths and parameters, with the exception of an additional periodic λ-swap move during the RETI simulations. Both methods approximated the free-energy gradient with respect to λ numerically, using the Zwanzig equation[13] and a value of $\Delta\lambda = 0.001$. Double-wide sampling[14] was used to check that this value of $\Delta\lambda$ was sufficiently small to ensure that the approximation was valid. After the data were collected, the free-energy gradients were integrated using the trapezium rule.[10] Ten million (10 M) steps of simulation were run at each value of λ for each leg of each mutation, with the relative free energy for each leg calculated over blocks of 0.5 M steps. The relative free energies stabilized within the first 3 M steps, so the final 7 M steps were used for data collection. The RETI simulations performed the λ-swap move every 50 000 (50 K) steps, with swaps only attempted between adjacent λ-replicas. No additional equilibration was necessary either before or after the λ-swap moves. Aside from these λ-swap moves, each RETI simulation was identical to its corresponding FDTI simulation.

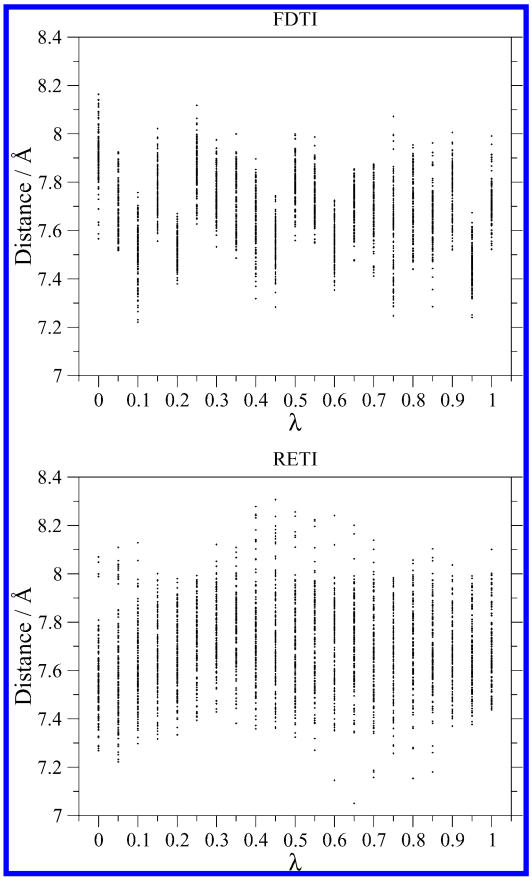

Figure 4. Distance between the C4 carbons on opposite phenyl rings of the calix[4]pyrrole derivative, as a function of λ, taken from the fluoride-to-chloride mutations, as calculated by FDTI and RETI. Distances were calculated every 50 000 (50 K) steps.

TABLE 1: Relative Free Energies for Each Leg, and Relative Binding Free Energies and Closure for Three Halides to a Calix[4]pyrrole Derivative, as Calculated by FDTI and RETI

	Relative Free Energy (kcal mol^{-1})	
leg	FDTI	RETI
	Fluoride to Chloride	
bound	34.8 (0.7)	34.1 (0.5)
free	16.1 (0.5)	16.9 (0.4)
binding	18.7 (0.8)	17.1 (0.7)
	Fluoride to Bromide	
bound	36.6 (0.8)	37.4 (0.7)
free	17.6 (0.6)	17.5 (0.5)
binding	19.1 (1.0)	20.0 (0.8)
	Chloride to Bromide	
bound	3.03 (0.06)	3.06 (0.05)
free	1.50 (0.04)	1.50 (0.03)
binding	1.52 (0.07)	1.56 (0.06)
	Closure	
bound	−1.1	0.3
free	−0.0	−0.9
binding	−1.1	1.3

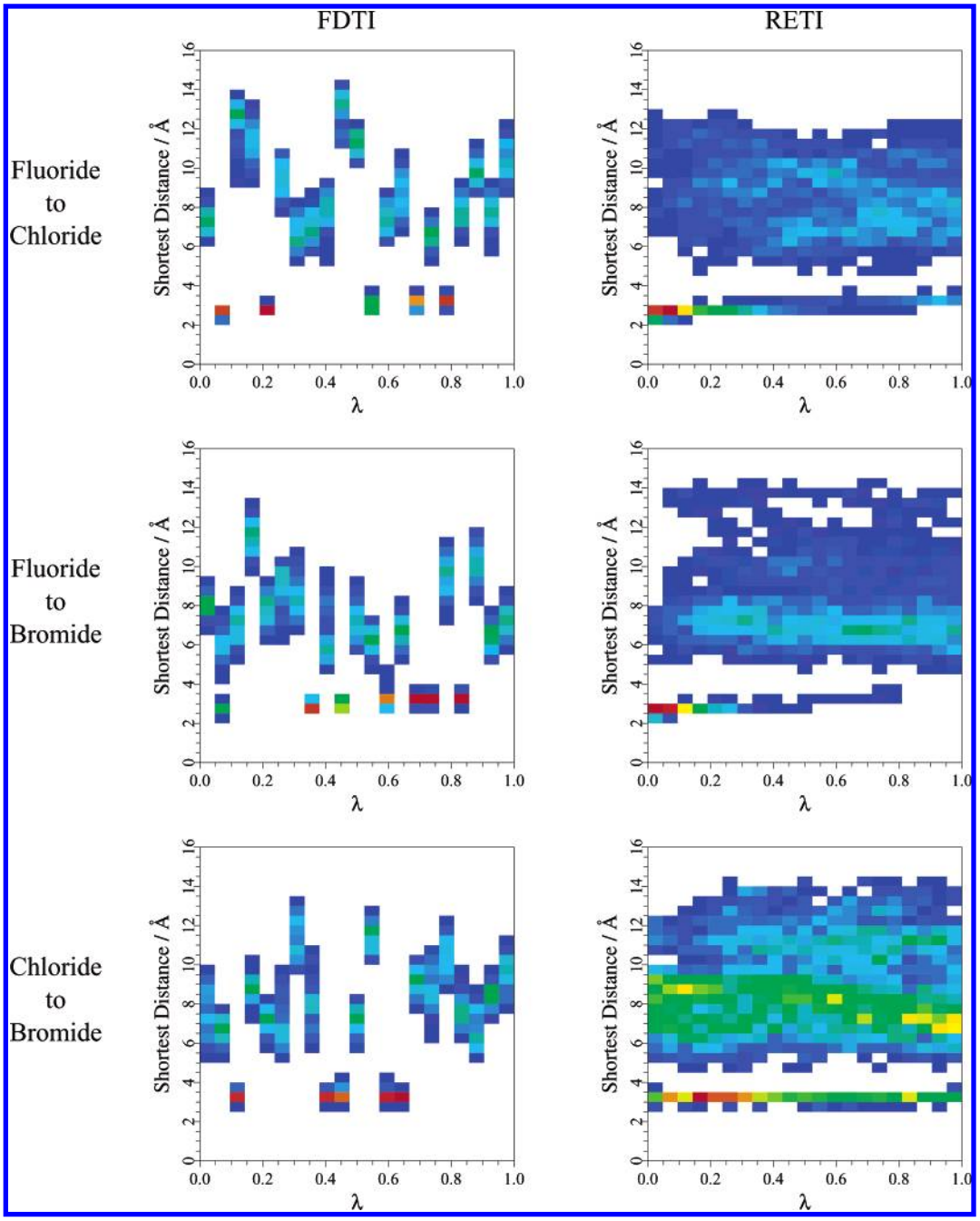

Figure 5. Shortest distance between the central halide and solvent water O atom, as a function of λ, from the free-leg simulations. Distances were calculated every 50 K MC steps and are histogrammed every 0.5 Å. The color scale runs from white (zero density), through blue (low density) and green (medium density) to red (high density).

4. Results

The free-energy results for each leg are shown in Table 1. The errors for each leg were determined by calculating batch averages of the free-energy gradient at each λ value every 500 K steps. The standard error of these averages was then integrated across the entire λ-coordinate to yield the maximum error. This analysis will overestimate the error but should be sufficiently sensitive to allow good comparison between FDTI and RETI. The relative binding free energies were calculated according to the free-energy cycle in Figure 1, and the error was calculated as the square root of the sum of the squares of the errors on the individual legs. The three mutations formed a closed cycle; therefore, the closure on each leg and on the relative binding free energies was also calculated as an additional estimate of error.

5. Analysis

5.1. Calculation of Binding Free Energies. The relative binding free energies of the ions show good agreement with those calculated for a similar calix[4]pyrrole system.[21] The relative binding free energies produced by FDTI and RETI show reasonable agreement with each other, with the errors on the RETI results being slightly smaller than those from FDTI.

In our previous work on this system,[20] the distances between pairs of atoms in the host were used to demonstrate that the configurational sampling of AdUmWHAM was greater than that for FEP. A similar analysis was performed on the trajectories produced via FDTI and RETI. The distances between pairs of atoms were calculated every 50 K steps and plotted with respect to λ. The distances between the C4 atoms of opposite phenyl

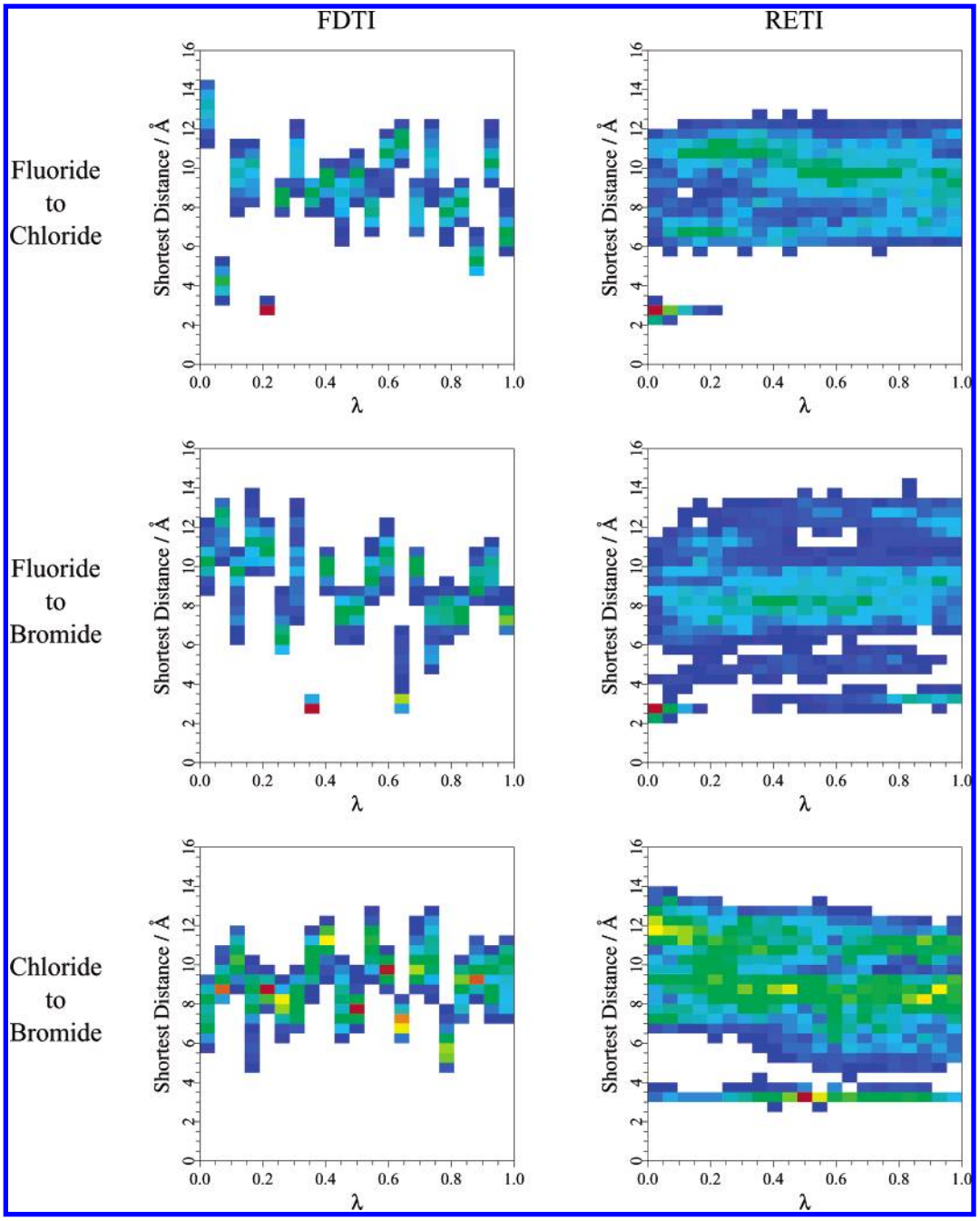

Figure 6. Shortest distance between the central halide and solvent water O atom, as a function of λ, from the bound-leg simulations. Distances were calculated every 50 K MC steps and are histogrammed every 0.5 Å. The color scale runs from white (zero density), through blue (low density) and green (medium density) to red (high density).

rings (see Figure 3) taken from the bound-leg fluoride to chloride mutation are shown in Figure 4.

These distances reveal that RETI has exhibited a greater range of configurational sampling than FDTI. FDTI seems to have become limited to sampling slightly different configurational substates at low λ, with the distances oscillating between mean values of 7.9 and 7.5 Å. In contrast, the dynamic λ-coordinate of RETI enables the trajectories to escape these minima, share information across the entire λ-coordinate, and thus sample more fully and more widely than FDTI. RETI exhibits the same advantages from using a dynamic λ-coordinate as does AdUmWHAM, without the problems of a Hamiltonian lag that have been identified in AdUmWHAM on other systems.[2]

5.2. Sampling of Contaminating Water. Previous work on this and related systems has demonstrated the importance of the contaminating waters in determination of the relative binding free energies of the halide ions.[20,21] To investigate the sampling of these waters during the FDTI and RETI simulations, the distances between the halide ion and the O atom of the closest water were calculated for configurations generated at each value of λ. These distances were calculated every 50 K steps and, to make the plot clearer, were histogrammed with a bin width of 0.5 Å. The distance histograms for each value of λ were combined together and renormalized into a single λ-distance histogram. Plots for each free-leg and bound-leg simulation are shown in Figures 5 and 6, respectively.

Each replica at each λ value started with a different random water distribution. These distributions can be classified into two types: distributions where a water was hydrogen-bonded to the halide, and distributions where the water was not hydrogen-bonded to the halide. Because of the low diffusion of the water through the DMSO solvent, the probability of a non-hydrogen-

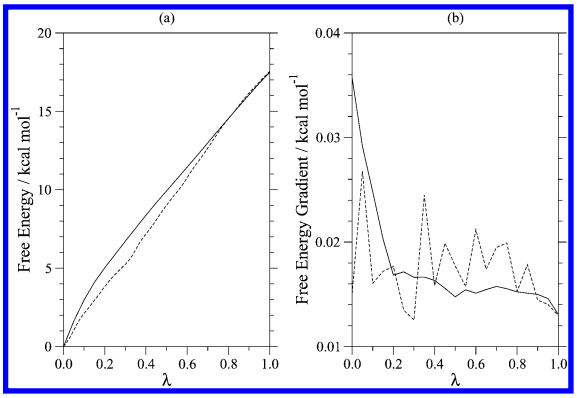

Figure 7. (a) Potential of mean force along λ for the free leg fluoride-to-bromide mutation, as calculated by (- - -) FDTI and (—) RETI. (b) Free-energy gradient across λ.

bonding distribution becoming a hydrogen-bonding distribution was very low. FDTI only samples a single replica at each λ value; therefore, the method effectively sampled from only a single water distribution at each λ value. Some of these distributions were hydrogen-bonding (seen in Figures 5 and 6 as points between 2 Å and 3 Å), whereas others were not. In contrast, the dynamic λ-coordinate of the RETI simulations allows each replica to move throughout the entire λ-coordinate. This allowed the statistics generated at each λ value to include the effects of multiple water distributions. The plots for RETI in Figures 5 and 6 thus show a wide range of distances at each λ value, with most λ values including sampling from both hydrogen-bonding and non-hydrogen-bonding water distributions. In addition to allowing each λ value to experience a range of water distributions, the λ-swap move is observed to have weighted the different water distributions across λ. The density of hydrogen-bonding water distributions is much higher at low values of λ for the fluoride-to-chloride and fluoride-to-bromide mutations. The λ-swap move can account for the fluoride's higher affinity for water and has swapped the hydrogen-bonding distributions down to low λ values. In contrast, there seems to be little difference in affinity for water between chloride and bromide, so the λ-swap move has distributed the hydrogen-bonding geometries more evenly over the entire λ-coordinate for the chloride-to-bromide mutations. The addition of the λ-swap move has improved the quality of sampling of the water distributions, because it has enabled each value of λ to experience multiple water distributions, and it has weighted the different distributions across λ. Thus, the relative binding free energies produced via RETI are of a higher quality than those from FDTI, because they include the effects of multiple water distributions and incorporate the higher affinity of fluoride for water. Because the improved sampling of water distibutions is the result of the swapping of multiple replicas to each λ value, improved results may be obtained by running more replicas, with fewer simulation steps per replica. As with other free-energy methods, prior knowledge of the system is required to judge the most-efficient number of replicas, with the smallest possible amount of sampling.

The effect of the improved water sampling is observed in the potentials of mean force (PMFs) predicted by RETI compared to those from FDTI. The PMF for the free-leg fluoride-to-bromide mutation is shown in Figure 7.

The PMF predicted by RETI consists of two distinct regions. The free energy increases more rapidly with λ at $\lambda < 0.2$ than at $\lambda > 0.2$. This can be visualized more clearly by plotting the gradient of the free energy with respect to λ, $(\Delta G/\Delta\lambda)_\lambda$, as calculated from the trajectories generated by the RETI simulation (see Figure 7). The free-energy gradient is high at low λ. Figure 5 shows that this corresponds to the region of λ where many hydrogen-bonding configurations were sampled. By defining a hydrogen-bonding configuration as one with a shortest halide-to-water O atom distance of <3.0 Å, the number of hydrogen-bonding configurations sampled at each value of λ could be counted and histogrammed, as shown in Figure 8. This plot shows a significant correlation between the density of hydrogen-bonding configurations and the free-energy gradient, which suggests that it is the distribution of hydrogen-bonding configurations that creates the two distinct regions in the PMF.

Considering the PMF generated by FDTI (see Figure 7), there is no clear pattern in the free-energy gradient across λ. The gradient seems to change randomly across λ, much like the distribution of hydrogen-bonding water distributions (see Figure 5). Indeed, the histogram of hydrogen-bonding configurations across λ (see Figure 8) shows a strong correlation between the free-energy gradient and the density of hydrogen-bonding water distributions.

The presence of water hydrogen-bonding to the halide increases the stability of the fluoride ion, compared to the other halides. This causes the increase in free-energy gradient that is observed in Figure 7. The λ-swap move of RETI enables the hydrogen-bonding water distributions to be moved to the correct region of λ, thus allowing RETI to approximate the true shape of the PMF better. In contrast, FDTI used a random distribution

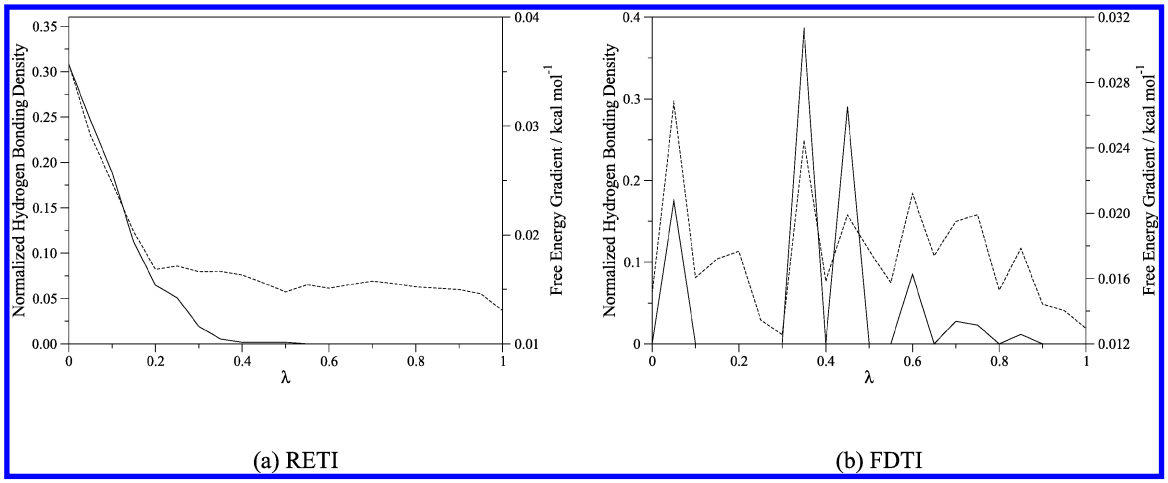

Figure 8. Free-energy gradient with respect to λ (- - -) for the free leg fluoride-to-bromide mutation, compared to (—) the density of halide-water hydrogen-bonding water distributions sampled at each value of λ, as calculated via (a) RETI and (b) FDTI.

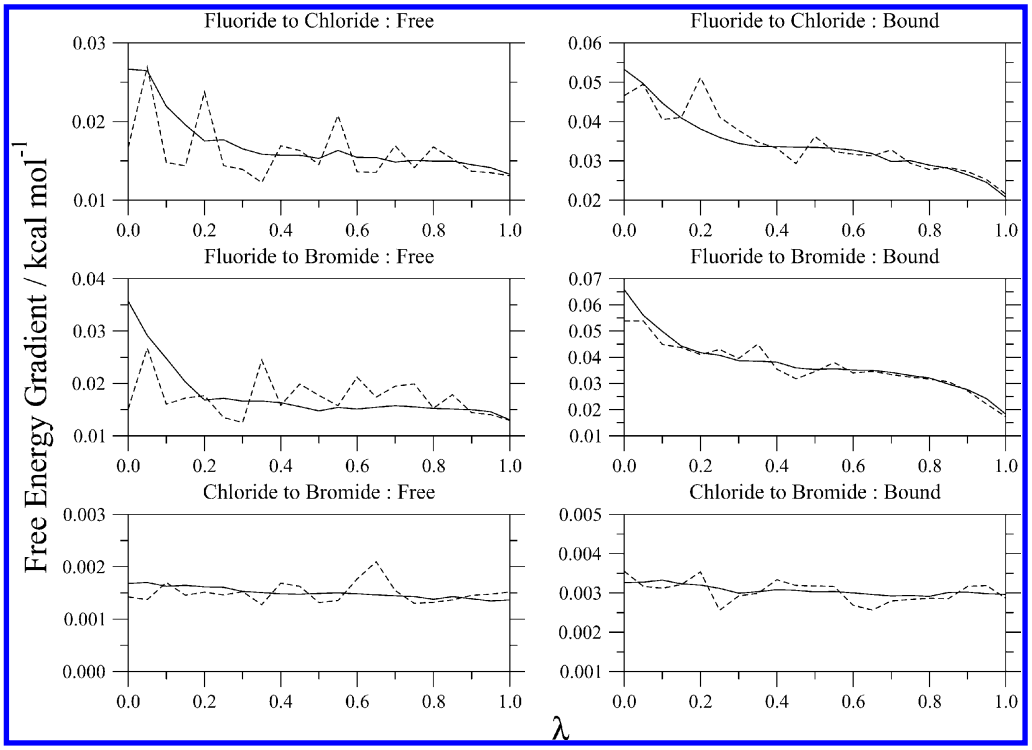

Figure 9. Free-energy gradient for each mutation, as calculated by (- - -) FDTI and (—) RETI.

of hydrogen-bonding water configurations across λ, which results in a randomly fluctuating free-energy gradient, and thus a poorer approximation of the shape of the PMF. It should, of course, be noted that RETI does not increase water sampling per se, but instead ensures that sampled configurations are appropriately distributed among the λ values. Methods for increasing the rate of solvent motion are being sought.

The effect of the improved water sampling of RETI is observed in the results of all the halide mutations (Figure 9).

The free-leg fluoride-to-chloride and fluoride-to-bromide mutations clearly show the increased free-energy gradient at low λ for RETI, compared to the randomly oscillating gradients from FDTI. The chloride-to-bromide mutation has a relatively constant gradient across λ, corresponding to the similar affinity of these two halides for water. The bound-leg mutations also show these same features, although to a lesser extent. The FDTI gradients oscillate but show the same increase at low λ as those calculated via RETI. Given that the FDTI hydrogen-bonding distribution is random across λ, this suggests that the increase in free-energy gradient is caused by some other factor (perhaps, for example, the configurational rearrangement of the host). In all mutations, RETI produces gradients that are more consistent across λ. Unlike FDTI, which produces gradients that seem to contain random error and fluctuate randomly across λ, RETI has produced gradients that vary smoothly across λ. This further suggests that the PMFs produced via RETI are of a higher quality than those produced via FDTI. This observation leads to the possibility that a RETI simulation may require fewer points along λ to be sampled, compared to FDTI.

6. Conclusion

The newly developed replica-exchange thermodynamic integration (RETI) method was tested and compared to finite difference thermodynamic integration (FDTI) on the calculation of the relative binding free energies of halides to a calix[4]-pyrrole derivative. The calculation was challenging, because the dimethylsulfoxide (DMSO) solvent included small amounts of contaminating water. The results demonstrate that RETI has many advantages over FDTI, because it was able to sample the effects of the contaminating water more fully. The λ-swap move of RETI enabled multiple water distributions to be sampled at each λ value and allowed the weighting of hydrogen-bonded water distributions toward the fluoride. The relative binding free energies produced via RETI thus included the effect of the fluoride's higher affinity for water, compared to the other halides. In addition, the use of the λ-swap move turned λ into a dynamic coordinate. This action resulted in the same improvements in configurational sampling of the host as those observed via the adaptive umbrella weigthed histogram analysis method (AdUmWHAM),[20] which also used a dynamic λ-coordinate. However, unlike AdUmWHAM, RETI achieved this without including any artifacts from the Hamiltonian lag that have been observed for this method on other systems.[2] As in its previous application,[2] RETI has demonstrated superior sampling, compared to FDTI, and has achieved this at effectively no additional computational expense.

Acknowledgment. We thank the BBSRC, EPSRC, Celltech, and the University of Southampton for funding this work, and Prof. W. L. Jorgensen for the provision of the MCPRO program and associated source code.

References and Notes

(1) Kollman, P. *Chem. Rev.* **1993**, *93*, 2395−2417.

(2) Woods, C. J.; King, M. A.; Essex, J. W. *J. Phys. Chem. B* **2003**, *107*, 13703−13710.

(3) Mezei, M. *J. Chem. Phys.* **1987**, *86*, 7084−7088.

(4) Guimaraes, C. R. W.; Alencastro, R. B. *Int. J. Quantum Chem.* **2001**, *85*, 713−726.

(5) Guimaraes, C. R. W.; Alencastro, R. B. *J. Med. Chem.* **2002**, *45*, 4995−5004.

(6) Guimaraes, C. R. W.; Alencastro, R. B. *J. Phys. Chem. B* **2002**, *106*, 466−476.

(7) Kamath, S.; Coutinho, E.; Desai, P. *J. Biomol. Struct. Dyn.* **1999**, *16*, 1239−1244.

(8) Reynolds, C. A.; King, P. M.; Richards, W. G. *Mol. Phys.* **1992**, *76*, 251−275.
(9) Chipot, C.; Pearlman, D. A. *Mol. Simulat.* **2002**, *28*, 1−12.
(10) Pearlman, D. A.; Charifson, P. S. *J. Med. Chem.* **2001**, *44*, 3417−3423.
(11) Oostenbrink, B. C.; Pitera, J. W.; Lipzig, M. M. H.; Meerman, J. H. N.; Van Gunsteren, W. F. *J. Med. Chem.* **2000**, *43*, 4594−4605.
(12) Barril, X.; Orozco, M.; Luque, F. J. *J. Med. Chem.* **1999**, *42*, 5110−5119.
(13) Zwanzig, R. W. *J. Chem. Phys.* **1954**, *22*, 1420−1426.
(14) Jorgensen, W. L.; Ravimohan, C. *J. Chem. Phys.* **1985**, *83*, 3050−3054.
(15) Sugita, Y.; Kitao, A.; Okamoto, Y. *J. Chem. Phys.* **2000**, *113*, 6042−6051.
(16) Fukunishi, H.; Watanabe, O.; Takada, S. *J. Chem. Phys.* **2002**, *116*, 9058−9067.
(17) Hansmann, U. H. E. *Chem. Phys. Lett.* **1997**, *281*, 140−150.
(18) Okabe, T.; Kawata, M.; Okamoto, Y.; Mikami, M. *Chem. Phys. Lett.* **2001**, *335*, 435−439.
(19) Camiolo, S.; Gale, P. A. *Chem. Commun.* **2000**, 1129−1130.
(20) Woods, C. J.; Camiolo, S.; Light, M. E.; Coles, S. J.; Hursthouse, M. B.; King, M. A.; Gale, P. A.; Essex, J. W. *J. Am. Chem. Soc.* **2002**, *124*, 8644−8652.
(21) Blas, J. R.; Marquez, M.; Sessler, J. L.; Luque, F. J.; Orozco, M. *J. Am. Chem. Soc.* **2002**, *124*, 12796−12805.
(22) Price, M. L. P.; Jorgensen, W. L. *J. Am. Chem. Soc.* **2000**, *122*, 9455−9466.
(23) Price, D. J.; Jorgensen, W. L. *Bioorg. Med. Chem. Lett.* **2000**, *10*, 2067−2070.
(24) Price, D. J.; Jorgensen, W. L. *J. Comput. Aid. Mol. Des.* **2001**, *15*, 681−695.
(25) Bartels, C.; Karplus, M. *J. Comput. Chem.* **1997**, *18*, 1450−1462.
(26) Kumar, S.; Payne, P. W.; Vasquez, M. *J. Comput. Chem.* **1996**, *17*, 1269−1275.
(27) van Hoorn, W. P.; Jorgensen, W. L. *J. Org. Chem.* **1999**, *64*, 7439−7444.
(28) Jorgensen, W. L.; Madura, J. D.; Swenson, C. J. *J. Am. Chem. Soc.* **1984**, *106*, 6638−6646.
(29) Jorgensen, W. L.; Maxwell, D. S.; Tirado-Rives, J. *J. Am. Chem. Soc.* **1996**, *118*, 11225−11236.
(30) Kaminski, G. A.; Jorgensen, W. L. *J. Phys. Chem. B* **1998**, *102*, 1787−1796.
(31) Jorgensen, W. L.; Chandrasekhar, J.; Madura, J. D.; Impey, R. W.; Klein, M. L. *J. Chem. Phys.* **1983**, *79*, 926−935.
(32) Jorgensen, W. L. MCPRO Version 1.5; Yale University: New Haven, CT, 1996.
(33) Owicki, J. C.; Scheraga, H. A. *Chem. Phys. Lett.* **1977**, *47*, 600−602.
(34) Jorgensen, W. L. *J. Phys. Chem.* **1983**, *87*, 5304−5314.